


An engineered T-cell engager with selectivity for high mesothelin-expressing cells and activity in the presence of soluble mesothelin

Daniel Snell , Tea Gunde, Stefan Warmuth, Bithi Chatterjee, Matthias Brock, Christian Hess, Maria Johansson, Alexandre Simonin, Fabio Mario Spiga, Christopher Weinert, Niels Kirk, Nicole Bassler, Lucia Campos Carrascosa, Naomi Flückiger, Robin Heiz, Sandro Wagen, Noreen Giezendanner, Alessandra Alberti, Yasemin Yaman, Dana Mahler, Dania Diem, Peter Lichtlen, and David Urech

Numab Therapeutics AG, Horgen, Switzerland

ABSTRACT

Mesothelin (MSLN) is an attractive immuno-oncology target, but the development of MSLN-targeting therapies has been impeded by tumor shedding of soluble MSLN (sMSLN), on-target off-tumor activity, and an immunosuppressive tumor microenvironment. We sought to engineer an antibody-based, MSLN-targeted T-cell engager (α MSLN/ α CD3) with enhanced ability to discriminate high MSLN-expressing tumors from normal tissue, and activity in the presence of sMSLN. We also studied the *in vivo* antitumor efficacy of this molecule (NM28-2746) alone and in combination with the multifunctional checkpoint inhibitor/T-cell co-activator NM21-1480 (α PD-L1/ α 4-1BB). Cytotoxicity and T-cell activation induced by NM28-2746 were studied in co-cultures of peripheral blood mononuclear cells and cell lines exhibiting different levels of MSLN expression, including in the presence of soluble MSLN. Xenotransplant models of human pancreatic cancer were used to study the inhibition of tumor growth and stimulation of T-cell infiltration into tumors induced by NM28-2746 alone and in combination with NM21-1480. The bivalent α MSLN T-cell engager NM28-2746 potently induced T-cell activation and T-cell mediated cytotoxicity of high MSLN-expressing cells but had much lower potency against low MSLN-expressing cells. A monovalent counterpart of NM28-2746 had much lower ability to discriminate high MSLN-expressing from low MSLN-expressing cells. The bivalent molecule retained this discriminant ability in the presence of high concentrations of sMSLN. In xenograft models, NM28-2746 exhibited significant tumor suppressing activity, which was significantly enhanced by combination therapy with NM21-1480. NM28-2746, alone or in combination with NM21-1480, may overcome shortcomings of previous MSLN-targeted immuno-oncology drugs, exhibiting enhanced discrimination of high MSLN-expressing cell activity in the presence of sMSLN.

ARTICLE HISTORY

Received 6 November 2022

Revised 13 June 2023

Accepted 2 July 2023

KEYWORDS

Antibody fragment; cancer immunotherapy; fusion protein; T-cell engager; T-cell stimulation; xenograft model

Introduction

Engineered bispecific antibodies with a paratope for a tumor antigen and another for CD3 were first shown in the 1980s to direct cytotoxic T cells to destroy cancer cells.^{1,2} Despite the early promise, only a few TCEs are currently in clinical use for oncologic indications, owing to on-target off-tumor toxicity, cytokine release syndrome, limited T-cell infiltration into the tumor, suboptimal potency, and an immunosuppressive tumor microenvironment.^{3,4} To address these challenges, researchers have developed numerous molecular formats to prolong plasma half-life, reduce on-target off-tumor toxicity, and increase specificity.^{3,4} For example, employing avidity-based binding to HER2 via a bivalent format was shown to improve the selective targeting (versus monovalent affinity-based binding) of HER2-overexpressing tumor cells over normal tissues expressing low levels of HER2.⁵ Currently, hundreds of T-cell-directed bispecific molecules employing a variety of molecular formats are in clinical trials.⁶

MSLN is an attractive immuno-oncology target as it is over-expressed in a number of solid tumors including mesothelioma, pancreatic cancer, ovarian cancer, endometrial cancer, non-small cell lung cancer, biliary cancer, and triple negative breast cancer.^{7,8} In triple-negative breast cancer, lung adenocarcinoma, pancreatic adenocarcinoma, and colorectal cancer, overexpression of MSLN correlates with poor prognosis or advanced pathologic stage.^{7,9–12} Furthermore, expression of MSLN in normal tissue is restricted to mesothelial cells lining the pleura, peritoneum, and pericardium.^{13–15} Two potential challenges associated with the use of MSLN as a target are expression in normal mesothelium and shedding of soluble MSLN into extracellular fluids, both of which could narrow the therapeutic window and reduce on-tumor target engagement.¹⁶ Bivalent MSLN binding, with its avidity-based characteristics, may offer a strategy to overcome some of these challenges and improve selectivity for high MSLN-expressing tumors.^{5,17}

CONTACT Daniel Snell  d.snell@numab.com  Numab Therapeutics AG, Bachtobelstrasse 5, Horgen CH-8810, Switzerland

© 2023 Numab Therapeutics AG. Published with license by Taylor & Francis Group, LLC.

This is an Open Access article distributed under the terms of the Creative Commons Attribution-NonCommercial License (<http://creativecommons.org/licenses/by-nc/4.0/>), which permits unrestricted non-commercial use, distribution, and reproduction in any medium, provided the original work is properly cited. The terms on which this article has been published allow the posting of the Accepted Manuscript in a repository by the author(s) or with their consent.

We have engineered a bispecific T-cell engager (TCE) that combines monovalent CD3 activation with bivalent MSLN binding. The goals driving molecular design choices included high selectivity for activation of T cells in the vicinity of high MSLN-expressing tumors over normal mesothelia, lack of systemic T-cell activation, a broad therapeutic window, lack of interference by soluble MSLN, high anti-tumor efficacy in MSLN-expressing tumors, and long plasma half-life. This report describes the proof-of-concept studies leading to the development of this TCE. We also explored its antitumor efficacy in combination with another bispecific molecule that simultaneously blocks the PD-1/PD-L1 checkpoint pathway and co-stimulates T cell activation through 4-1BB.

Materials and methods

Ethics

All mouse experiments and protocols were approved by the animal welfare body at Charles River Discovery Services North Carolina and the associated local authorities and were conducted according to all applicable international, national, and local laws and guidelines. For studies using human PBMCs, donors provided written informed consent and blood samples were collected, anonymized, and used according to ethical approval from Blutspende Zurich (BASEC Nr. Req 2020-00983).

Molecule design and production

Complementarity-determining regions (CDRs) from rabbit antibodies targeting human MSLN, CD3 epsilon, and serum albumin were grafted onto a stability-promoting human variable domain acceptor scaffold in which framework region 4 (FR4) of the kappa-type light chain was replaced by a lambda-type FR4 (see Egan et al.,¹⁸ resulting in λ capped antibody Fvs and single-chain Fvs. The three target-specific variable domains were assembled into the trispecific, trivalent single-chain (sc) MATCH3 antibody format (NM28-1872) or into the trispecific, tetravalent MATCH4 antibody format (NM28-2746). See Table 1 for a guide to the MATCH molecules used in this study. The polypeptide chains were expressed in CHO cells and clarified from the cell supernatant by standard capture and polishing processes. NM21-1480 and its mouse analog (NM21-1601) were produced as described previously.¹⁹

MSLN expression density

MSLN expression density was quantified using either a phycoerythrin (PE)-labeled α MSLN antibody (clone C-3,

Santa Cruz Biotechnology) or an in-house DyLight488-labeled α MSLN antibody (clone 7D9.v3). Receptor density values are reported as antibody-binding capacity (ABC), which was derived from standard curves generated with Quantum Simply Cellular beads anti-mouse or anti-human IgG (Bangs Laboratories, Inc.). Beads and test samples were stained according to the manufacturer's instructions with the corresponding saturating concentration of α MSLN antibody. To calculate ABC, the geometric means for the four Quantum Simply Cellular bead populations were analyzed using FlowJo software (BD Biosciences). The QuickCal v2.3 Excel spreadsheet-based analysis template (Bangs Laboratories, Inc.) was used to create a standard curve using linear regression. R-square values were typically ≥ 0.99 . Values for the test samples were interpolated from the standard curve.

In vitro cytotoxicity and T cell activation

Human peripheral blood mononuclear cells (PBMCs) were isolated from buffy coats of human blood samples, which were then separated by density gradient centrifugation using SepMate tubes with Lymphoprep (StemCell Technologies) and following the manufacturer's instructions. H226 and MeT5A cells were obtained from ATCC (#CRL-5826; 9444), and C86 mesothelial cells from Coriell Institute (#AG07086).

PBMCs were cocultured for 40 h with cell lines of interest at an effector-to-target ratio (E:T) of 30:1 in the presence of test reagents (highest concentration 50 nM in 5 \times dilution steps for a total of 11 concentration points including untreated), human serum albumin (25 mg/mL), and with or without soluble mesothelin (sMSLN; PeproTech). After 40 h, 100 μ L of supernatant was aspirated and tested for lactate dehydrogenase (LDH) activity using the Cytotoxicity Detection Kit from Roche, which is based on measurement of the activity of LDH released from the cytosol of damaged cells into the supernatant. The remaining supernatant was collected and frozen at -80°C for downstream multiplexed cytokine analysis.

For assays of T-cell activation, cells were labeled with (all from Biolegend): Fixable live/dead Aqua, anti-human CD4 APC-Cy7 (clone OKT4), anti-human CD11c PE-Cy7 (clone Bu15), anti-human CD8 PerCP-Cy5.5 (clone SK1), and anti-human CD69 PE (clone FN50). Cells were assayed on a flow cytometer (Attune NxT, ThermoFisher Scientific), and analyzed using FlowJo software (BD Biosciences) and GraphPad Prism (Version 9.3.1) for the upregulation of CD69 as a measure of both CD4 and CD8 T cell activation.

Table 1. A guide to the MATCH antibody-based molecules described in this study.

α MSLN/ α CD3/ α HSA T-cell engagers (all monovalent for CD3 and HSA)	
NM28-2746	Bivalent for MSLN (MATCH4)
NM28-1872	Monovalent for MSLN (MATCH3)
α PD-1/ α 4-1BB/ α HSA ¹⁹ Checkpoint inhibitor and T-cell co-stimulator (all monovalent)	
NM21-1480	Human analog (MATCH3)
NM21-1601	Mouse analog (anti-serum albumin-binding moiety recognizes mouse serum albumin; anti-PD-1 and anti-4-1BB moieties same as NM21-1480) (MATCH3)

In vitro cytokine secretion

In vitro cytokine secretion was measured on cell supernatants from cytotoxicity assays using BioLegend Cytometric Bead Array (CBA) flow cytometric assay and following the manufacturer's instructions. Samples were counted on a flow cytometer (Attune NxT, ThermoFisher Scientific) and analyzed using BioLegend's cloud-based LegendPLEX Data Analysis Software and GraphPad Prism (Version 9.3.1).

In vitro cytotoxicity by real-time cell imaging

Human PBMCs were isolated as described above. Pan T cells were isolated from PBMCs using the Pan T cell isolation kit from Miltenyi Biotec and following the manufacturer's instructions.

Target cell lines of interest were transduced with IncuCyte NuLight Red Lentivirus Reagent (EF1 α , Puro). Briefly, the cells were seeded in antibiotic-free media at 10,000 cells/well and left to attach overnight at 37°C. NuLight Red Lentivirus was added at a MOI (multiplicity of infection) of 3 and Polybrene (Sigma) at 8 μ g/mL. After 24 h, media was removed and selection media containing Puromycin was added and incubated for additional 72–96 h. Efficiency of target cell transduction was evaluated using the SX5IncuCyte (Sartorius), a live-cell imaging instrument.

Transduced NuLight Red target cells were then co-cultured with isolated pan T cells for up to 6 d at an effector-to-target ratio (E:T) of 5:1 in the presence of different compounds at different concentrations, human serum albumin (25 mg/mL), and IncuCyte Cytotox Green reagent or CellEvent Caspase 3/7 detection reagent. Cytotoxicity was assessed using the IncuCyte SX5. Plates were scanned with a 10 \times objective every 3 h for 6 d. Cell death was quantified by assessment of the number of NuLight Red-transduced target cells remaining in culture or by detection of Cytotox Green or Caspase 3/7 signal normalized to target cell count. Data were analyzed using the integrated IncuCyte S5X Software and GraphPad Prism (Version 9.3.1).

Mouse xenotransplant model of human pancreatic cancer

Female NCG mice (NOD-Prkdc^{em26Cd52}Il2rg^{em26Cd22}/NjuCrl, Charles River) were 9-week old, with body weights (BWs) ranging from 17 to 24 g on Day 1 of the study. Human HPAC pancreatic adenocarcinoma cell lines (HPAC; American Type Culture Collection) were harvested during exponential growth and resuspended in a 50% MatrigelTM (BD Biosciences) and phosphate-buffered saline (PBS) mixture in the presence or absence of PBMCs. On day 1, all animals were injected subcutaneously in the right flank (0.2 mL/mouse), with either HPAC cells alone (1×10^7 cells) or HPAC cells with human PBMCs (2.5×10^6 cells). Tumor growth was monitored twice weekly using a caliper in two dimensions. Treatments were administered intravenously beginning on day 5 and subsequently every 5 days for seven consecutive dosings (day 35). All treatments were administered in fixed volumes of 0.1 mL/mouse and 0.05

ml/mouse. Control IgG treatment was palivizumab (Synagis, purchased from a regional pharmacy; 0.02 mg/animal), a clinically available antibody with specific binding to an irrelevant antigen (respiratory syncytial virus protein F). On day 40, mice were sacrificed under anesthesia and tumors excised.

Tumor samples were dissociated according to the gentleMACSTM Dissociator protocol (Tumor Dissociation Kit, Miltenyi Biotec), filtered through a 70 micron cell strainer and rinsed twice in PBS/2% FBS. The final cell suspensions were prepared in PBS at pH 7.4 at 1×10^7 cells/mL and kept on ice. Cell suspensions (100 μ L) were added into 96-well plates and stained for 15 min at 4°C with 100 μ L of reconstituted Live/Dead Aqua (Life Technologies) following the manufacturer's instructions. After two washes with 150 μ L of staining buffer, Fc receptors were blocked using Mouse & Human TruStain FcX, Fc γ RIV (Biolegend) in 50 μ L volume for 10 min on ice before immunostaining. Cells were stained for 30 min at 4°C with 50 μ L of staining buffer containing antibodies (50 μ L). Cells were washed twice with 150 μ L of staining buffer and resuspended in 230 μ L of staining buffer for analysis. The antibody panel included antibodies for CD45, TCR β , CD4, and CD8. Flow cytometry was performed on a BD LSRFortessa and analyzed with FlowJo software (Tree Star, Inc.).

Results

A bivalent MSLN-targeting T-cell engager constructed on MATCH molecular scaffolding

The MSLN-targeted T-cell engagers (α MSLN-TCEs) described here are recombinant antibodies constructed using MATCHTM (Multispecific Antibody-based Therapeutics by Cognate Heterodimerization) technology (Figure 1a).¹⁸ The final multi-specific drug candidate (NM28-2746) is a heterodimeric molecule comprising two protein chains with inter-domain Gly4-Ser linkers connecting the variable heavy (V_H) and variable light (V_L) domains. As shown in Figure 1b, one protein chain contains one α MSLN-binding variable region fragment (Fv) in a single-chain Fv (scFv) format linked to the light chain of the second α MSLN Fv, and the light chain of the α CD3 Fv. The second protein chain contains an anti-human serum albumin (α hSA) scFv linked to the heavy chain of the α CD3 Fv, and the heavy chain of the second α MSLN Fv. An interchain disulfide bond links the two protein chains after cognate pairing of the split variable α hSA and α CD3 regions in the core of the protein. Figure 1c shows a structural model of NM28-2746, a bivalent α MSLN-TCE. Figure 1d demonstrates that the final product of NM28-2746 synthesis (see Methods) eluted as a single peak on size-exclusion HPLC.

Avidity-based binding provides greater discrimination of high MSLN-expressing cells than affinity-based binding

A major goal of molecular design was to optimize on-tumor, MSLN-dependent, T-cell activation while minimizing on-target off-tumor T-cell activation in order to 1) optimize the

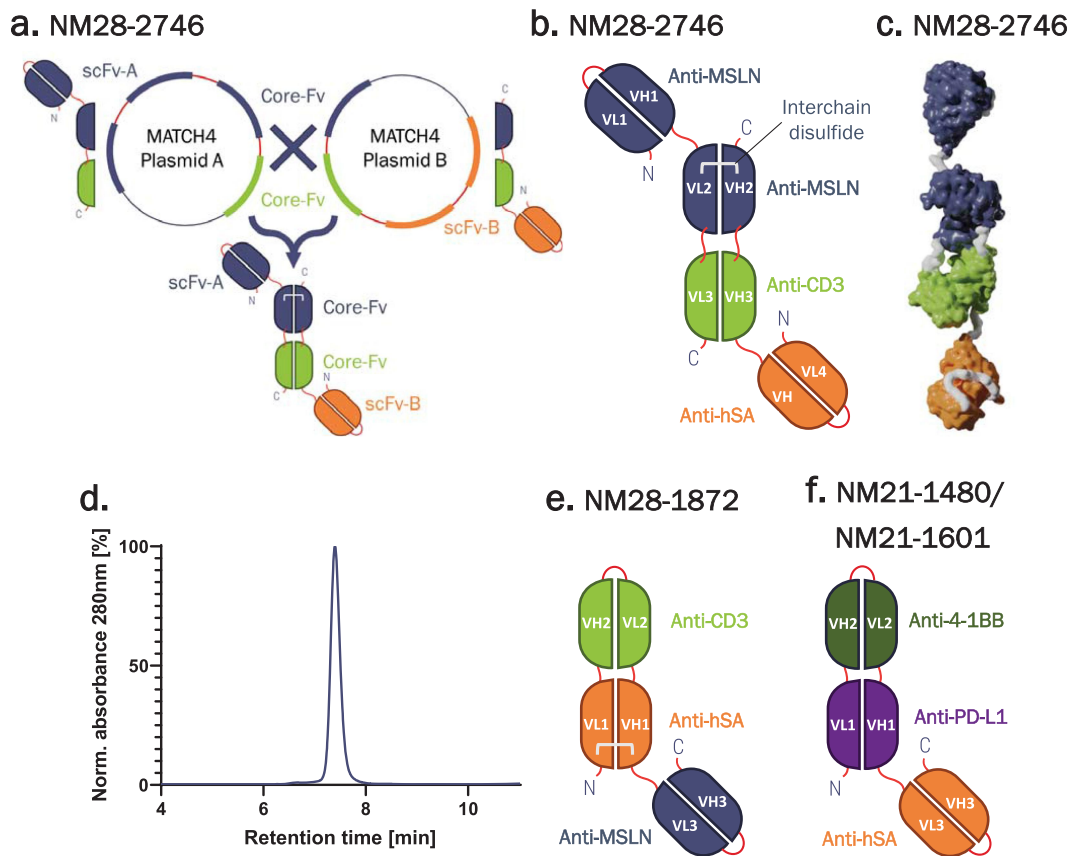


Figure 1. Composition and structure of the bivalent α MSLN TCE, NM28-2746. (a) NM28-2746 is a MATCH4™ (multispecific antibody-based therapeutics by cognate heterodimerization) molecule formed from two polypeptide chains. (b) Schematic representation of the molecular scaffold of the two protein chains of NM28-2746 showing the interchain disulfide bond and the final assembly of subunits. Gly4-Ser linkers are shown in red. (c) Structural model of NM28-2746 prepared using BIOVIA discovery studio software. (d) Representative SE-HPLC chromatogram of the final product of NM28-2746 production. (e) Schematic representation of the monovalent α MSLN TCE NM28-1872. (f) Schematic representation of the human checkpoint inhibitor/T-cell co-stimulator NM21-1480 and its mouse-appropriate analog NM21-1601 (see text and Table 1).

drug's therapeutic window and 2) minimize the effects of soluble MSLN on drug activity. An established strategy to achieve such goals is the use of avidity-based antibody binding rather than affinity-based binding.^{5,17}

To test the avidity-based design strategy, we constructed a bivalent α MSLN TCE (NM28-2746) and a monovalent α MSLN TCE (NM28-1872; Figure 1e). Immune-mediated cytotoxicity of the bivalent and monovalent TCEs was studied across three cell lines having different levels of MSLN expression (Figure 2a,b): H226 lung cancer cells and two immortalized, nonmalignant mesothelial cell lines, MeT5a and LP-9/Coriell 86 cells. Cells were cultured together with PBMCs at an effector-to-target ratio (E:T) of 30:1, and cytotoxicity was assessed during 40 h of exposure to different concentrations of bivalent α MSLN (NM28-2746) or monovalent α MSLN (NM28-1872) TCEs. As shown by the example in Figure 2c (left panel), bivalent NM28-2746 induced cytotoxicity with an EC_{50} in the low picomolar range. Similar results were observed in experiments using pan-T-cells instead of PBMCs (data not shown). Additionally, experiments using PBMCs depleted of T cells demonstrated no cytotoxic effect (data not shown). Furthermore, the EC_{50} and maximum effect size were both strongly influenced by MSLN expression levels such that the potency of NM28-2746-induced cytotoxicity was 3–10–

fold higher in high MSLN-expressing (H226) cells compared with low MSLN-expressing (Met5a and C86) cells. Henceforth, we will refer to this difference as the “discrimination window,” in reference to the ability of the TCE to discriminate between high- and low-MSLN-expressing cells or tissues. In the same set of experiments, co-cultures treated with the monovalent NM28-1872 exhibited cytotoxicity with >10-fold lower potency than the bivalent molecule, and with a much narrower discrimination window (Figure 2c, right panel).

In this same series of experiments, we also evaluated the effects of NM28-2746 and NM28-1872 on activation of CD8+ T cells and secretion of selected cytokines. Bivalent NM28-2746 induced a dose-dependent activation of CD8+ T cells that was dependent on MSLN density of the cell line (Figure 2d, left panel). In contrast, monovalent NM28-1872 induced CD8+ T-cell activation less potently and with a narrower discrimination window (Figure 2d, right panel). Figure 2e summarizes the EC_{50} and E_{max} values from the experiments of Figure 2c-d. The dose-response curves for cytokine secretion (Figure 2f) were consistent with the results of T-cell activation with regard to the discrimination window. We did observe, however, that both α MSLN TCEs induced higher IL-1b secretion in the C86 co-cultures than in Met5a co-cultures (Figure 2f, left

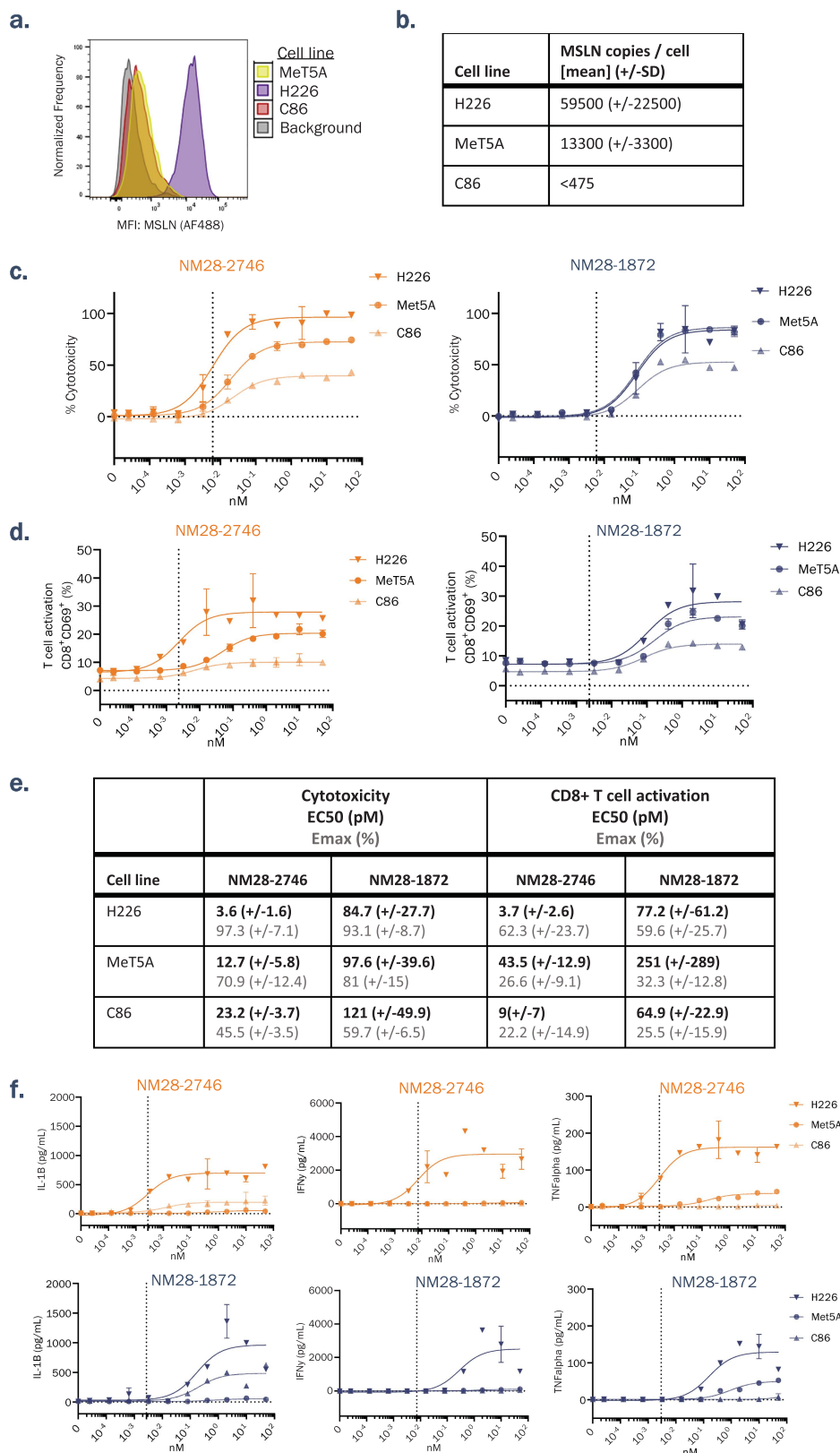


Figure 2. Discrimination of high MSLN-expressing cells from low MSLN-expressing cells: a bivalent α MSLN TCE versus its monovalent counterpart. (a) Distribution of MSLN density in three human cell lines used in subsequent experiments: H226 lung cancer cells, and two immortalized nonmalignant mesothelial cell lines, MeT5a, and LP-9/Coriell 86 cells. (b) Mean (SD) MSLN density in the three cell lines shown in a. (c) Dose-dependent cytotoxicity, as determined by LDH assay, after 40 h of exposure to the bivalent α MSLN TCE NM28-2746 (left) and its monovalent counterpart NM28-1872 (right) in co-cultures of the indicated cells and human PBMCs (E:T, 30:1). Values are mean \pm SD of replicates from a representative experiment. In co-cultures of CHO cells (which lack MSLN expression) and human PBMCs, NM28-2746 exhibited no cytotoxicity (not shown). The discrimination window (see text) for cytotoxicity in high MSLN-expressing H226 cells versus low MSLN-expressing C86 cells (fold change [ratio] of EC₅₀) was 9.91 (geometric mean of three independent experiments), and the corresponding value for the monovalent NM28-1872 was 1.24 (geometric mean of 5 independent experiments). (d) Dose-dependent CD8+ T-cell activation as determined by CD69 flow cytometry in the same experiment as c. Values are mean \pm SD of replicates from a representative experiment. (e) Mean (SD) EC₅₀ and E_{max} values from at least three experiments represented in c and d. (f) Dose-dependent cytokine release in the same experiment as parts c and d.

panels); we suspect this observation may be due to stimulation of IL-1b release from the C86 cells by T-cell-derived cytokines, rather than the IL-1b coming directly from the T cells.²⁰ Together, the results of all three outcome measures (cytotoxicity, CD8+ T-cell activation, and cytokine release) illustrate that the potency of the bivalent α MSLN TCE NM28-2746 was strongly dependent on MSLN expression in the target cells, whereas the potency of the monovalent α MSLN TCE NM28-1872 exhibited much less dependence on MSLN expression.

The dose-dependent cytotoxicity was further investigated over 7 days using the InCuCyte real-time cell imaging platform. Addition of NM28-2746 or NM28-1872 to the culture media resulted in dose- and time-dependent changes in the percentage of living cells (Figure 3a). The difference in potency of the two TCEs across cell lines is shown graphically in Figure 3b, which plots the AUC (day 0 to day 6) of the viable cell counts as a function of dose. In H226 cells, bivalent NM28-2746 had an EC_{50} of 0.2 pM, whereas monovalent NM28-1872 had an EC_{50} 25-fold higher (5 pM). In MeT5a cells, in contrast, the EC_{50} s of the two molecules were more similar.

The bivalent α MSLN TCE NM28-2746 maintains a broad discrimination window in the presence of high levels of soluble MSLN

One of the challenges of using MSLN as a target for tumor-directed therapies is the presence of soluble MSLN (sMSLN) in the extracellular space.^{16,21} We explored how sMSLN affects cytotoxicity of the bivalent and monovalent TCEs by repeating the LDH-based cytotoxicity assays. As shown in Figure 4, increasing concentrations of sMSLN in the culture media shifted the cytotoxic EC_{50} of bivalent NM28-2746 from about 1 pM (no sMSLN) to about 35 pM (500 ng/mL sMSLN). Importantly, however, the broad discrimination window for NM28-2746 was maintained even in the presence of high concentrations of sMSLN. In contrast, monovalent NM28-1872 consistently exhibited a narrow discrimination window.

Combination of the α MSLN TCE with PD-L1 blockade and T-cell co-stimulation enhances antitumor efficacy in a xenograft model of human pancreatic cancer

Previous attempts to develop MSLN-targeting immunotherapies for cancer have reported limited efficacy, due

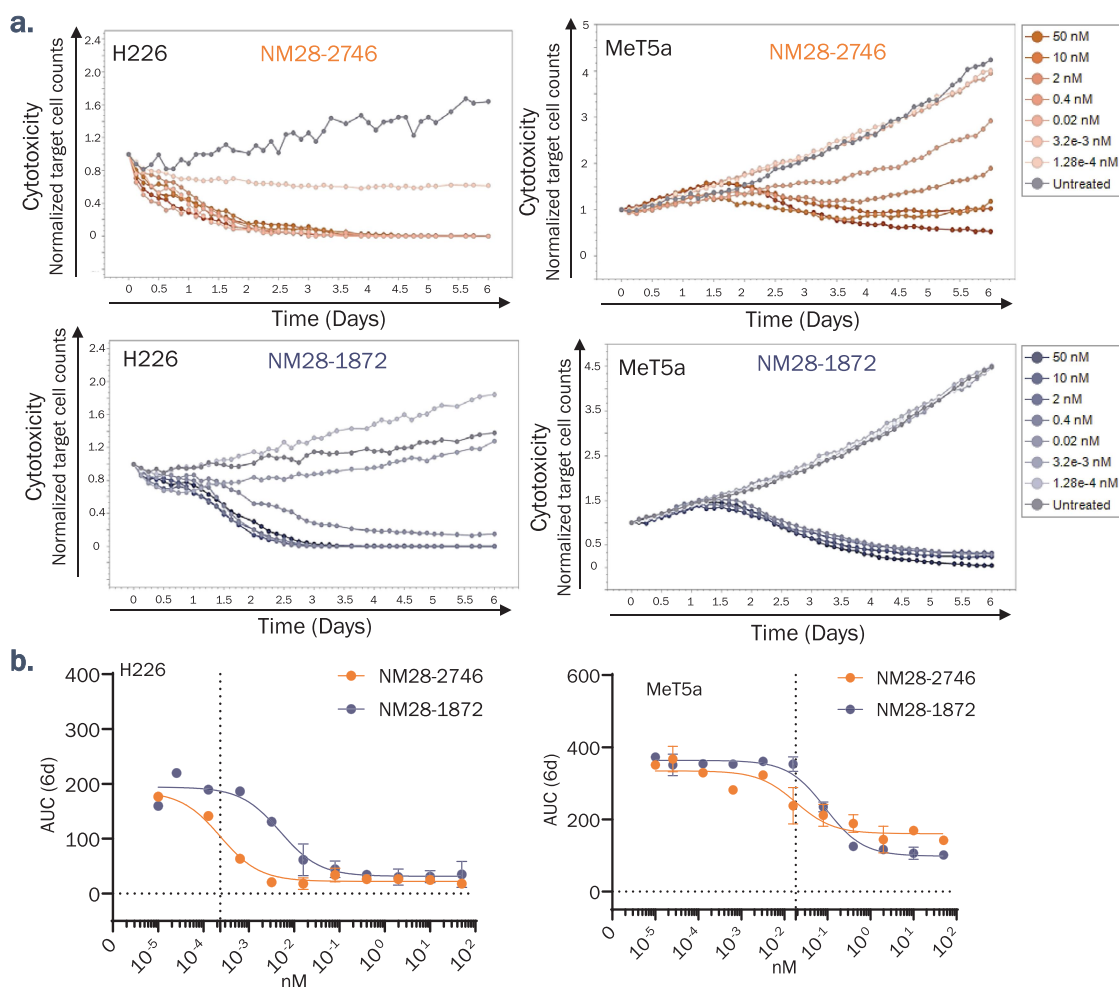


Figure 3. Dose- and time-dependence of cytotoxicity induced by NM28-2746 or NM28-1872 as measured by real-time live-cell imaging of NuLight-Red labeled H226 or MeT5a cells. (a) Time-course of viable target-cell counts during treatment with various doses of NM28-2746, NM28-1872, or control (untreated). Target cells were co-cultured (E:T, 5:1) with pan T cells. (b) Integrated area-under-the-curve (AOC) from day 0 to day 6 from the experiment in a. Vertical dashed line indicates the EC_{50} for NM28-2746.

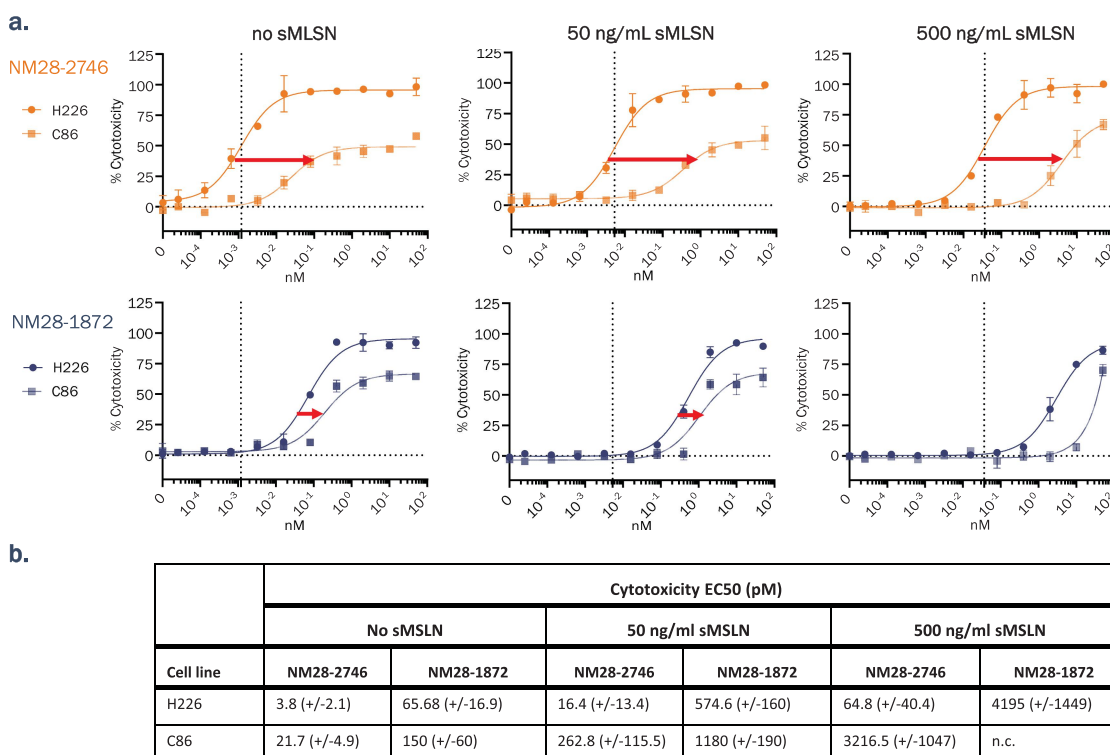


Figure 4. Effects of soluble mesothelin (sMSLN) on α MSLN TCE-induced cytotoxicity. (a) Effects of sMSLN on NM28-2746 (orange)- and NM28-1872 (gray)-induced cytotoxicity in H226 cells and C86 cells co-cultured with human PBMCs (E:T, 30:1) for 40 h. Cells were co-cultured with the indicated amounts of sMSLN, and cytotoxicity was assessed by LDH assay. Red arrow indicates the magnitude of the discrimination window (see text). Vertical dashed line indicates the EC₅₀ value for NM28-2746 in H226 cells. Values are mean \pm SD of replicates from one experiment of at least 2. (b) Mean (SD) EC₅₀ values from at least two experiments represented in a.

at least in part to an immunosuppressive tumor microenvironment.³ Early evidence suggests that combining MSLN-targeting immunotherapies with PD-1/PD-L1 blockade may improve antitumor efficacy,^{22–26} though recent evidence suggests that it may be necessary to overcome multiple mechanisms of T-cell anergy.²⁷ Therefore, we tested the antitumor efficacy of the bivalent α MSLN TCE NM28-2746 in combination with a mouse-appropriate analog (NM21-1601) of the next-generation checkpoint inhibitor, NM21-1480 (see Introduction and Table 1).¹⁹ In co-cultures of H226 cells and human pan-T cells, combination treatment with NM28-2746 and NM21-1480 produced substantially greater H226 cytotoxicity than either antibody alone (Figure 5a).

This combination treatment was then studied in immunocompromised mice (Female NCG mice) xenografted with human pancreatic cancer (HPAC) cells. Figure 5b demonstrates that the HPAC cells grown in co-culture with human PBMCs were sensitive to cytotoxicity during treatment with the α MSLN TCE NM28-2746 in a dose-dependent manner, with an EC₅₀ of 23 pM. In the mouse xenograft experiments, NM28-2746 alone inhibited tumor growth in a dose-dependent manner (Figure 5c-d top row), reaching statistically significant effects for the 1 mg/kg dose (at day 40). The α PD-L1/ α 4-1BB molecule, NM21-1601, did not significantly inhibit tumor growth alone at the single dose studied (1 mg/kg; Figure 5c-d lower row, left-most panel). The combination of the two molecules inhibited tumor growth in a manner that was dependent on the dose of NM28-2746 (at a constant 1 mg/kg dose of NM21-1601) and was statistically significant even at the lowest

dose (0.008 mg/kg; Figure 5c-d lower row, right three panels) at day 40.

Combination therapy remodels the tumor microenvironment toward a cytotoxic milieu

At the end of the treatment period (Day 40) of the preceding experiments, tumors were excised, dissociated, and evaluated for T-cell infiltration by flow cytometry. As shown in Figure 6, animals treated with the α MSLN TCE exhibited intratumoral T-cell infiltration with predominately CD8⁺ T cells. The addition of the α PD-L1/ α 4-1BB molecule further promoted CD8⁺ T-cell infiltration into the tumor. These results suggest that the treatments exerted a change in the tumor microenvironment toward a more cytotoxic milieu, consistent with the effects on tumor volume shown in the preceding figure (Figure 5) and with CD8⁺ T-cell activation shown *in vitro* (Figure 2d).

Discussion

Mesothelin was identified as an attractive target for cancer immunotherapy in the 1990s,¹⁴ and numerous MSLN-targeting immunotherapies are currently in development.¹⁵ Despite intense interest, the antitumor efficacy of many MSLN-targeted therapies has been modest or disappointing, and some had safety concerns. We have developed a bivalent α MSLN MATCH-based TCE, currently designated NM28-2746, which exhibited more potent activity than its monovalent counterpart in cell-based cytotoxicity assays and xenograft models of human pancreatic cancer.

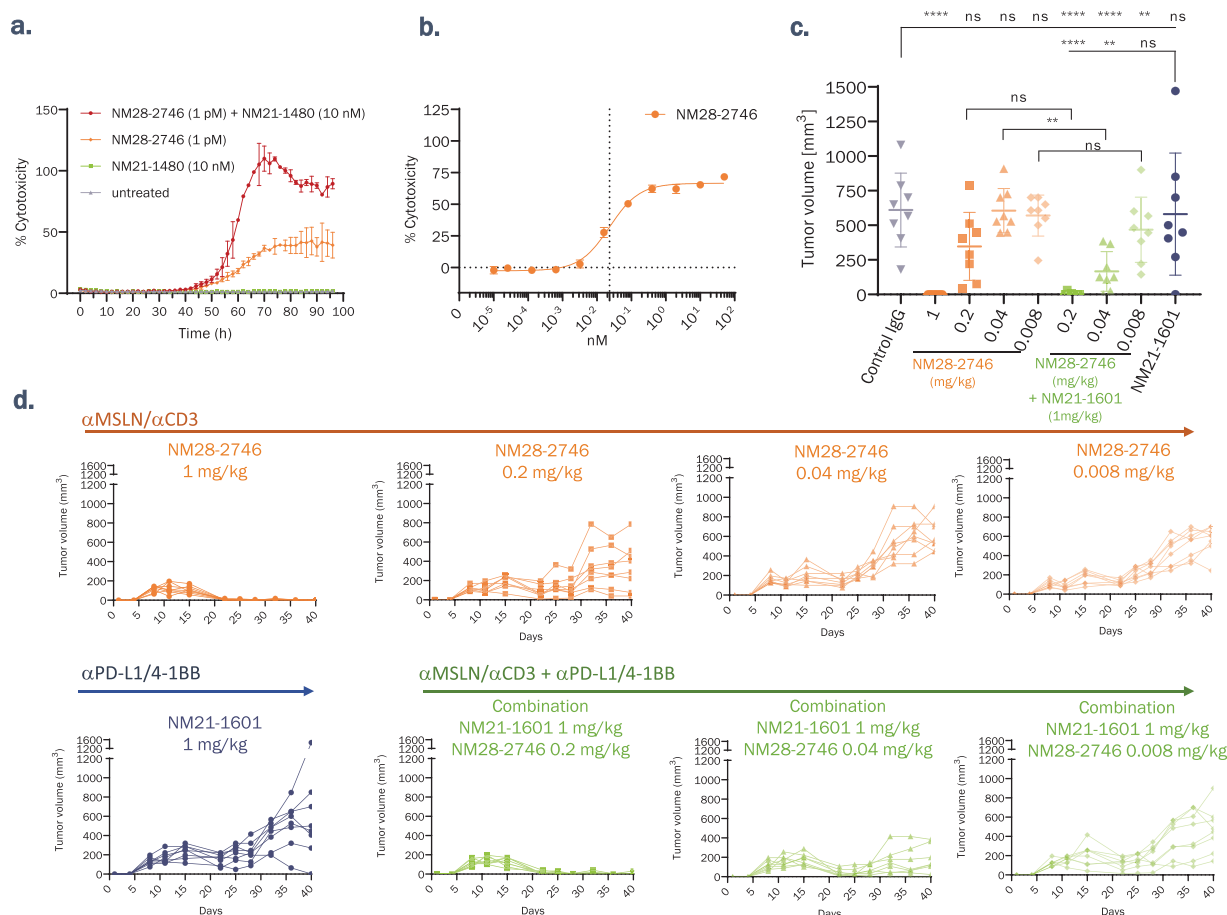


Figure 5. Combination therapy with the α MSLN TCE NM28-2746 and the α PD-L1-blocker/4-1BB agonist NM21-1601 (a mouse analog of NM21-1480). (a) Percent cytotoxicity (mean \pm SD) of H226 cells in co-culture with pan-T cells after treatment with NM28-2746 (1 pM), NM21-1480 (10 nM), or the combination. (b) Dose-response curve for NM28-2746-induced cytotoxicity in human PDAC cells in culture. (c) Tumor volume on day 40 in NGC mice xenotransplanted with human PDAC cells and PBMCs, and treated once every 5 days with the indicated agents and combinations. Control IgG was palivizumab (0.02 mg/animal). Each marker represents one animal. Error bars indicate means \pm SD. Statistical analysis by one-way ANOVA followed by Tukey's multiple comparisons test. ns: not significant; * p < 0.01; ** p < 0.01; *** p < 0.001; **** p < 0.0001. (d) Tumor volume as a function of time after engraftment for each animal.

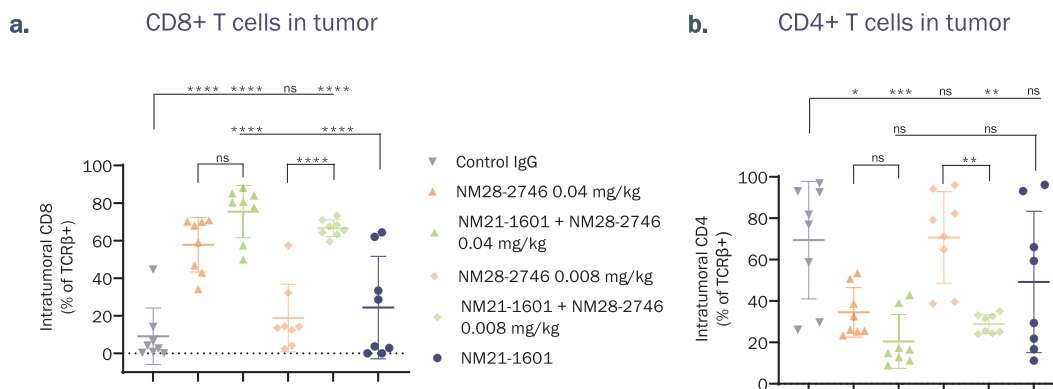


Figure 6. Tumor-infiltrated T-cell populations at day 40 in treated xenografts. CD8+ (a) and CD4+ (b) T-cell counts as a percentage of TCR β + cell counts at day 40 in the tumors from animals depicted in Figure 5. Markers indicate individual animals and error bars indicate mean \pm SD. Control IgG was palivizumab (0.02 mg/animal). Statistical analysis by one-way ANOVA followed by Tukey's multiple comparisons test. ns: not significant; * p < 0.01; ** p < 0.01; *** p < 0.001; **** p < 0.0001.

With increased efficacy of T-cell-activating therapies, there is also increased potential for systemic activation of T cells or on-target off-tumor activity.^{8,28} Our experiments showed that the bivalent α MSLN TCE had 3–10-fold higher potency against high MSLN-expressing tumor cells as compared with low MSLN-expressing cells derived from human mesothelium. Furthermore, the bivalent molecule had more than 10-fold

greater potency than its monovalent counterpart. These results are consistent with previous studies using bivalent avidity-based molecules for target recognition,^{5,17} as well as with studies using monovalent affinity-based α MSLN molecules, the latter of which showed little discrimination of targets on the basis of MSLN density.²⁹ The improved efficacy of NM28-2746 and its ability to discriminate high MSLN-expressing cells

from low MSLN-expressing cells warrant continued study of this molecule.

Shedding of soluble MSLN from MSLN-expressing tumors has been shown to impair the efficacy of MSLN-targeting immunotherapies.^{21,30,31} Strategies to combat this problem have included small-molecule inhibitors of MSLN sheddases and antibodies to the protease-sensitive regions of membrane-bound MSLN.^{16,21} We have demonstrated that the bivalent molecule NM28-2746—but not its monovalent counterpart—retained its wide discrimination window in the presence of high concentrations of sMSLN. It has not been reported whether other MSLN-targeting therapeutics exhibit corresponding properties.^{17,29}

Many TCEs have exhibited only limited ability to overcome an immunosuppressive tumor microenvironment.^{3,4,32} Indeed, upregulation of tumoral PD-L1 is commonly observed during T-cell activating immunotherapy.^{23,33–37} It has been suggested that combining a T-cell-activating bispecific drug with immune checkpoint inhibitors may be a viable strategy to overcome this problem.^{3,4,38} Preclinical studies have supported this strategy,^{23,34–36,39–41} and it is being studied in several clinical trials.³ However, Schreiner et al.²⁷ noted that blockade of PD-1/PD-L1 interaction may be insufficient. Our studies of combination therapy support this view. Using mice xenografted with human PDACs, we combined three modalities of lymphocyte stimulation – CD3 activation, PD-L1 inhibition, and 4-1BB co-stimulation – by using two molecular therapies: the α MSLN TCE NM28-2746 and a mouse version of the bifunctional, trispecific molecule NM21-1480.¹⁹ This combination showed superior efficacy to either agent alone in this model. Furthermore, the increased recruitment of CD8+ T cells into the tumor microenvironment suggests that this improved efficacy was a result of increased recruitment and activation of cytotoxic T cells.

Previous studies have shown that the bifunctionality of the α PD-L1/ α 4-1BB antibody NM21-1480 (and by extrapolation its mouse analog NM21-1601) is a key feature of its antitumor efficacy. Specifically, the ability of NM21-1480 to activate T cells through 4-1BB is strongly dependent on the anchoring function of its α PD-L1 moiety; T-cell activation was much less potent when 4-1BB binding and PD-L1 binding were mediated by independent antibodies.¹⁹

In the current studies, NM28-2746 potently stimulated release of T-cell-derived cytokines, which could potentially enhance the immune response in the tumor microenvironment. On the other hand, systemic cytokine release syndrome (CRS) has been a persistent problem associated with the use of TCEs in the past.³ In the clinic, therapies with the potential to induce CRS are often administered with step-wise dosing to minimize the risk and severity of CRS.⁴² A proposed molecular design strategy for addressing this problem involves carefully adjusting the affinity of the CD3-binding domain of the TCE.⁴³ The clinical effectiveness of this strategy is not yet established.

Together, the results of our studies demonstrate that it may be possible to overcome many of the challenges that have hampered the clinical development of α MSLN TCEs for solid tumors. The results support the clinical development of NM28-2746 in patients with MSLN-positive tumors, for whom better treatment options are needed.

Acknowledgments

Scientific writing support was provided by Ken Scholz, PhD.

Disclosure statement

All authors are employees of Numab Therapeutics AG. Research and manuscript preparation supported by Numab Therapeutics AG.

Funding

Research and manuscript preparation supported by Numab Therapeutics AG.

ORCID

Daniel Snell  <http://orcid.org/0000-0003-0107-4821>

Data availability statement

Due to the nature of the research and due to legal and commercial reasons, supporting data is not available.

References

- Perez P, Hoffman RW, Shaw S, Bluestone JA, Segal DM. Specific targeting of cytotoxic T cells by anti-T3 linked to anti-target cell antibody. *Nature*. 1985;316(6026):354–356. doi:10.1038/316354a0.
- Staerz UD, Kanagawa O, Bevan MJ. Hybrid antibodies can target sites for attack by T cells. *Nature*. 1985;314(6012):628–631. doi:10.1038/314628a0.
- Middelburg J, Kemper K, Engelberts P, Labrijn AF, Schuurman J, van Hall T. Overcoming challenges for CD3-Bispecific antibody therapy in solid tumors. *Cancers Basel*. 2021;13(2):287. doi:10.3390/cancers13020287.
- Singh A, Dees S, Grewal IS. Overcoming the challenges associated with CD3+ T-cell redirection in cancer. *Br J Cancer*. 2021;124(6):1037–1048. doi:10.1038/s41416-020-01225-5.
- Slaga D, Ellerman D, Lombana TN, Vij R, Li J, Hristopoulos M, Clark R, Johnston J, Shelton A, Mai E, et al. Avidity-based binding to HER2 results in selective killing of HER2-overexpressing cells by anti-HER2/CD3. *Sci Transl Med*. 2018;10(463). doi:10.1126/scitranslmed.aat5775.
- Wang S, Chen K, Lei Q, Ma P, Yuan AQ, Zhao Y, Jiang Y, Fang H, Xing S, Fang Y, et al. The state of the art of bispecific antibodies for treating human malignancies. *EMBO Mol Med*. 2021;13(9):e14291. doi:10.15252/emmm.202114291.
- Weidemann S, Gagelmann P, Gorbokov N, Lennartz M, Menz A, Luebke AM, Kluth M, Hube-Magg C, Blessin NC, Fraune C, et al. Mesothelin expression in human tumors: A tissue microarray study on 12,679 tumors. *Biomedicines*. 2021;9(4):397. doi:10.3390/biomedicines9040397.
- Hassan R, Thomas A, Alewine C, Le DT, Jaffee EM, Pastan I. Mesothelin immunotherapy for cancer: Ready for prime time? *J Clin Oncol*. 2016;34(34):4171–4179. doi:10.1200/JCO.2016.68.3672.
- Kachala SS, Bograd AJ, Villena-Vargas J, Suzuki K, Servais EL, Kadota K, Chou J, Sima CS, Vertes E, Rusch VW, et al. Mesothelin overexpression is a marker of tumor aggressiveness and is associated with reduced recurrence-free and overall survival in early-stage lung adenocarcinoma. *Clin Cancer Res*. 2014;20(4):1020–1028. doi:10.1158/1078-0432.CCR-13-1862.
- Thomas A, Chen Y, Steinberg SM, Luo J, Pack S, Raffeld M, Abdullaev Z, Alewine C, Rajan A, Giaccone G, et al. High mesothelin expression in advanced lung adenocarcinoma is associated with

- KRAS mutations and a poor prognosis. *Oncotarget*. 2015;6(13):11694–11703. doi:10.18632/oncotarget.3429.
11. Tozbikian G, Brogi E, Kadota K, Catalano J, Akram M, Patil S, Ho AY, Reis-Filho JS, Weigelt B, Norton L, et al. Mesothelin expression in triple negative breast carcinomas correlates significantly with basal-like phenotype, distant metastases and decreased survival. *PLoS One*. 2014;9(12):e114900. doi:10.1371/journal.pone.0114900.
 12. Winter JM, Tang LH, Klimstra DS, Brennan MF, Brody JR, Rocha FG, Jia X, Qin L-X, D'Angelica MI, DeMatteo RP, et al. A novel survival-based tissue microarray of pancreatic cancer validates MUC1 and mesothelin as biomarkers. *PLoS One*. 2012;7(7):e40157. doi:10.1371/journal.pone.0040157.
 13. Chang K, Pastan I, Willingham MC. Isolation and characterization of a monoclonal antibody, K1, reactive with ovarian cancers and normal mesothelium. *Int J Cancer*. 1992;50(3):373–381. doi:10.1002/ijc.2910500308.
 14. Pastan I, Hassan R. Discovery of mesothelin and exploiting it as a target for immunotherapy. *Cancer Res*. 2014;74(11):2907–2912. doi:10.1158/0008-5472.CAN-14-0337.
 15. Faust JR, Hamill D, Kolb EA, Gopalakrishnapillai A, Barwe SP. Mesothelin: An immunotherapeutic target beyond solid tumors. *Cancers Basel*. 2022;14(6):1550. doi:10.3390/cancers14061550.
 16. Zhang Y, Chertov O, Zhang J, Hassan R, Pastan I. Cytotoxic activity of immunotoxin SS1P is modulated by TACE-dependent mesothelin shedding. *Cancer Res*. 2011;71(17):5915–5922. doi:10.1158/0008-5472.CAN-11-0466.
 17. Yoon A, Lee S, Lee S, Lim S, Park Y-Y, Song E, Kim D-S, Kim K, Lim Y. A novel T cell-engaging bispecific antibody for treating mesothelin-positive solid tumors. *Biomolecules*. 2020;10(3):399. doi:10.3390/biom10030399.
 18. Egan TJ, Diem D, Weldon R, Neumann T, Meyer S, Urech DM. Novel multispecific heterodimeric antibody format allowing modular assembly of variable domain fragments. *MAbs*. 2017;9(1):68–84. doi:10.1080/19420862.2016.1248012.
 19. Warmuth S, Gunde T, Snell D, Brock M, Weinert C, Simonin A, Hess C, Tietz J, Johansson M, Spiga FM, et al. Engineering of a trispecific tumor-targeted immunotherapy incorporating 4-1BB co-stimulation and PD-L1 blockade. *Oncoimmunology*. 2021;10(1):2004661. doi:10.1080/2162402X.2021.2004661.
 20. Douvdevani A, Rapoport J, Konforty A, Argov S, Ovnat A, Chaimovitz C. Human peritoneal mesothelial cells synthesize IL-1 α and β . *Kidney Int*. 1994;46(4):993–1001. doi:10.1038/ki.1994.359.
 21. Liu X, Onda M, Watson N, Hassan R, Ho M, Bera TK, Wei J, Chakraborty A, Beers R, Zhou Q, et al. Highly active CAR T cells that bind to a juxtamembrane region of mesothelin and are not blocked by shed mesothelin. *Proc Natl Acad Sci USA*. 2022;119(19):e2202439119. doi:10.1073/pnas.2202439119.
 22. Chong EA, Melenhorst JJ, Lacey SF, Ambrose DE, Gonzalez V, Levine BL, June CH, Schuster SJ. PD-1 blockade modulates chimeric antigen receptor (CAR)-modified T cells: refueling the CAR. *Blood*. 2017;129(8):1039–1041. doi:10.1182/blood-2016-09-738245.
 23. Sam J, Colombetti S, Fauti T, Roller A, Biehl M, Fahrni L, Nicolini V, Perro M, Nayak T, Bommer E, et al. Combination of T-Cell bispecific antibodies with PD-L1 checkpoint inhibition elicits superior anti-tumor activity. *Front Oncol*. 2020;10:575737. doi:10.3389/fonc.2020.575737.
 24. Adusumilli PS, Zauderer MG, Rivière I, Solomon SB, Rusch VW, O'Ceirbhail RE, Zhu A, Cheema W, Chintala NK, Halton E, et al. A Phase I trial of regional mesothelin-targeted CAR T-cell therapy in patients with malignant pleural disease, in combination with the Anti-PD-1 agent pembrolizumab. *Cancer Discov*. 2021;11(11):2748–2763. doi:10.1158/2159-8290.CD-21-0407.
 25. Liu G, Zhang Q, Li D, Zhang L, Gu Z, Liu J, Liu G, Yang M, Gu J, Cui X, et al. PD-1 silencing improves anti-tumor activities of human mesothelin-targeted CAR T cells. *Hum Immunol*. 2021;82(2):130–138. doi:10.1016/j.humimm.2020.12.002.
 26. Wang Z, Li N, Feng K, Chen M, Zhang Y, Liu Y, Yang Q, Nie J, Tang N, Zhang X, et al. Phase I study of CAR-T cells with PD-1 and TCR disruption in mesothelin-positive solid tumors. *Cell Mol Immunol*. 2021;18(9):2188–2198. doi:10.1038/s41423-021-00749-x.
 27. Schreiner J, Thommen DS, Herzig P, Bacac M, Klein C, Roller A, Belousov A, Levitsky V, Savic S, Moersig W, et al. Expression of inhibitory receptors on intratumoral T cells modulates the activity of a T cell-bispecific antibody targeting folate receptor. *Oncoimmunology*. 2016;5(2):e1062969. doi:10.1080/2162402X.2015.1062969.
 28. Hagerty BL, Pegna GJ, Xu J, Tai C-H, Alewine C. Mesothelin-Targeted recombinant immunotoxins for solid tumors. *Biomolecules*. 2020;10(7):973. doi:10.3390/biom10070973.
 29. Molloy ME, Austin RJ, Lemon BD, Aaron WH, Ganti V, Jones A, Jones SD, Strobel KL, Patnaik P, Sexton K, et al. Preclinical characterization of HPN536, a trispecific, T-Cell-Activating protein construct for the treatment of mesothelin-expressing solid tumors. *Clin Cancer Res*. 2021;27(5):1452–1462. doi:10.1158/1078-0432.CCR-20-3392.
 30. Zhang J, Qiu S, Zhang Y, Merino M, Fetsch P, Avital I, Filie A, Pastan I, Hassan R. Loss of mesothelin expression by mesothelioma cells grown in vitro determines sensitivity to anti-mesothelin immunotoxin SS1P. *Anticancer Res*. 2012;32:5151–5158.
 31. Awuah P, Bera TK, Folivi M, Chertov O, Pastan I. Reduced shedding of surface mesothelin improves efficacy of mesothelin-targeting recombinant immunotoxins. *Mol Cancer Ther*. 2016;15(7):1648–1655. doi:10.1158/1535-7163.MCT-15-0863.
 32. Zhou S, Liu M, Ren F, Meng X, Yu J. The landscape of bispecific T cell engager in cancer treatment. *Biomark Res*. 2021;9(1):38. doi:10.1186/s40364-021-00294-9.
 33. Köhnke T, Krupka C, Tischer J, Knösel T, Subklewe M. Increase of PD-L1 expressing B-precursor ALL cells in a patient resistant to the CD19/CD3-bispecific T cell engager antibody blinatumomab. *J Hematol Oncol*. 2015;8(1):111. doi:10.1186/s13045-015-0213-6.
 34. Krupka C, Kufer P, Kischel R, Zugmaier G, Lichtenegger FS, Köhnke T, Vick B, Jeremias I, Metzeler KH, Altmann T, et al. Blockade of the PD-1/PD-L1 axis augments lysis of AML cells by the CD33/CD3 BiTE antibody construct AMG 330: reversing a T-cell-induced immune escape mechanism. *Leukemia*. 2016;30(2):484–491. doi:10.1038/leu.2015.214.
 35. Laszlo GS, Gudgeon CJ, Harrington KH, Walter RB. T-cell ligands modulate the cytolytic activity of the CD33/CD3 BiTE antibody construct, AMG 330. *Blood Cancer J*. 2015;5(8):e340. doi:10.1038/bcj.2015.68.
 36. Osada T, Patel SP, Hammond SA, Osada K, Morse MA, Lyster HK. CEA/CD3-bispecific T cell-engaging (BiTE) antibody-mediated T lymphocyte cytotoxicity maximized by inhibition of both PD1 and PD-L1. *Cancer Immunol Immunother*. 2015;64(6):677–688. doi:10.1007/s00262-015-1671-y.
 37. Herrmann M, Krupka C, Deiser K, Brauchle B, Marcinek A, Ogrinc Wagner A, Rataj F, Mocikat R, Metzeler KH, Spiekermann K, et al. Bifunctional PD-1 \times α CD3 \times α CD33 fusion protein reverses adaptive immune escape in acute myeloid leukemia. *Blood*. 2018;132(23):2484–2494. doi:10.1182/blood-2018-05-849802.
 38. Kobold S, Pantelyushin S, Rataj F, Vom Berg J. Rationale for combining bispecific T cell activating antibodies with checkpoint blockade for cancer therapy. *Front Oncol*. 2018;8:285. doi:10.3389/fonc.2018.00285.
 39. Chen N, Morello A, Tano Z, Adusumilli PS. CAR T-cell intrinsic PD-1 checkpoint blockade: A two-in-one approach for solid tumor immunotherapy. *Oncoimmunology*. 2017;6(2):e1273302. doi:10.1080/2162402X.2016.1273302.

40. Cherkassky L, Morello A, Villena-Vargas J, Feng Y, Dimitrov DS, Jones DR, Sadelain M, Adusumilli PS. Human CAR T cells with cell-intrinsic PD-1 checkpoint blockade resist tumor-mediated inhibition. *J Clin Invest.* 2016;126(8):3130–3144. doi:10.1172/JCI83092.
41. Crawford A, Haber L, Kelly MP, Vazzana K, Canova L, Ram P, Pawashe A, Finney J, Jalal S, Chiu D, et al. A mucin 16 bispecific T cell-engaging antibody for the treatment of ovarian cancer. *Sci Transl Med.* 2019;11(497). doi:10.1126/scitranslmed.aau7534.
42. Tian Z, Liu M, Zhang Y, Wang X. Bispecific T cell engagers: an emerging therapy for management of hematologic malignancies. *J Hematol Oncol.* 2021;14(1):75. doi:10.1186/s13045-021-01084-4.
43. Haber L, Olson K, Kelly MP, Crawford A, DiLillo DJ, Tavaré R, Ullman E, Mao S, Canova L, Sineshchekova O, et al. Generation of T-cell-redirecting bispecific antibodies with differentiated profiles of cytokine release and biodistribution by CD3 affinity tuning. *Sci Rep.* 2021;11(1):14397. doi:10.1038/s41598-021-93842-0.